Received 25 July 2022, accepted 12 August 2022, date of publication 17 August 2022, date of current version 29 August 2022.
Digital Object Identifier 10.1109/ACCESS.2022.3199422

RESEARCH ARTICLE

Day-Ahead Scheduling of Integrated Power and Water System Considering a Refined Model of Power-to-Gas

DONGSEN LI[1], CIWEI GAO[1], (Senior Member, IEEE), TAO CHEN[1,2], (Member, IEEE), JUAN ZUO[3], AND XINHONG WU[4]
[1]School of Electrical Engineering, Southeast University, Nanjing 210096, China
[2]Jiangsu Provincial Key Laboratory of Smart Grid Technology and Equipment, Southeast University, Nanjing 210096, China
[3]Department of Virtual Power Plant Laboratory, State Grid Shanghai Interconnection Research Institute Company Ltd., Shanghai 201210, China
[4]Department of Sales and Energy Data Center, State Grid Zhejiang Integrated Energy Service Company, Hangzhou 310016, China

Corresponding author: Ciwei Gao (ciwei.gao@seu.edu.cn)

This work was supported by the State Grid Corporation of China Project under Grant 5100-202119574A-0-5-SF.

ABSTRACT To accommodate surplus electricity and decarbonize, power-to-gas (PtG) is being widely considered in the integrated energy system with high proportion of renewable energy. However, the reaction model of PtG should be refined for the sake of making a precise operation strategy and economic evaluation. Compared with the ordinary model of power-to-gas process, this article makes two main improvements. First, an explicit expression of electrolytic process is given according to the usage of electricity. In the refined electrolytic model, the recovery of the extra heat in the electrolytic process and the compression of feed-in gas is explored. Second, the response model of the methanation process to the intermittency of the renewable energy is established. Considering the increasing coupling of power system and water network, we formulate a day-ahead scheduling program for an integrated power and water system (IPWS). Thus, the role of double regulation of power-to-gas is more noticeable. Finally, the accuracy and economical performance of the refined model of power-to-gas is demonstrated through case studies. The results show a significant body of recoverable extra heat reaching 26.6% of the total power consumption. Also, it shows a dramatic growth in PtG's consumption by 61.9% considering compression consumption. Moreover, the information gap decision theory (IGDT) is applied in the unit commitment scheme. Based on IGDT, the impact of the renewable energy uncertainty on the decision-making of IPWS operator is discussed.

INDEX TERMS Power-to-gas, integrated power and water system, refined model, intermittency, information gap decision theory.

NOMENCLATURE

A. VARIABLES

$f_{\mathrm{CH_4}}$	The produced methane, m^3
ΔH_{PtG}	Reaction heat of ptg, kw
P_{in}	The input power, kw
$H_{\mathrm{PtG,CH_4}}$	Heat dissipation per unit power consumption, kw
P_{PtG}	The power consumption of ptg, kw
$\mathrm{U_{HHV}}$	Higher-heating-value voltage, V
T	Temperature, K
U_{cell}	Cell voltage, V
P_{ele}	Power used to produce hydrogen and heat, kw
$P^t_{ele,\mathrm{Dis}}$	The heat dissipation in heat transmission, kw
$P^t_{ele,\mathrm{Rec}}$	The extra heat of the electrolyser, kw
τ_{res}	The restart time, s
Π_{idle}	The idle state duration, min
u_{idle}	The idle phase, 0-1
u_{on}	The on state, 0-1
u_{start}	The start-up state
u_{stand}	The state with a stand-by load
n	The molar flow of the gas, -

The associate editor coordinating the review of this manuscript and approving it for publication was Shafi K. Khadem.

C_{op}	Operation cost of IPWS, CNY
R_{op}	The revenue of IPWS, CNY
c	Price, CNY/kwh
t	Time, h
P_{CFU}	Unit power of CFU, kw
P_{GFU}	Unit power of GFU, kw
D	Carbon emission quota of RIES, t
E	Actual carbon emission, t
ff_{PtG}	The produced gas by ptg, m^3
$\mathrm{H}_{\mathrm{PtG}}$	The released heat by ptg, kw
d	Node water load, m^3/h
q	Water flow in pipe, m^3/h
H_{out}	The outlet tank hydraulic head, m
h_{pi}	Head losses in water pipes, kw
h_{va}	Head losses in valves, kw
h_{pu}	Pumping heads of the pump stations, m
$\Delta T_{start-up}$	The start-up period
ΔT_{idle}	The idle duration
ΔT_{int}	The intermittent period

B. CONSTANTS

η_{ele}	The efficiency of water electrolysis, -
$\varepsilon_{\mathrm{CH_4}}$	Stoichiometric coefficient, -
$\upsilon_{\mathrm{H_2}}$	Conversion rate, Nm^3/kwh^{-1}
$\rho_{\mathrm{H_2}}$	Density of hydrogen, g/m^3
M_{H_2}	Molar mass, g/mol
$\eta_{\mathrm{PtG}}^{\mathrm{CH_4/h}}$	The proportion of reaction heat used for heating, -
η_{E}	The electrolyzer efficiency, -
N_{stack}	The number of electrolytic cells, -
i_{cell}	The current density, A/m^2
S_{act}	The active area of each electrolytic cell, m^2
C	The overall thermal capacity, kj/K
T_{amb}	The ambient temperature, K
R_{the}	The overall thermal resistance, K/kw
Z	The compressibility factor, -
R_{gas}	The molar ideal gas constant, -
γ	The heat capacity ratio, -
η_{com}	The compression efficiency, -
N_{com}	The number of compressors, -
p_{in}, p_{out}	The pressure at the inlet/outlet, bar
$\widetilde{P}_{\mathrm{WT}}$	The forecasted output of wind power, kw
$\mu_{\mathrm{PtG,CO_2}}$	Coefficient of carbon dioxide needed for methanation, -
$\Xi_{tran,PDN}$	Power distribution fee, CNY/kwh
$\Xi_{tran,WDN}$	Water distribution fee, CNY/m^3
$\Xi_{\text{fe-WT}}$	Feed-in tariff of wind power, CNY/kwh
$\Xi_{\text{fe-CFU}}$	Feed-in tariff of CFU, CNY/kwh
$\Xi_{\text{fe-GFU}}$	Feed-in tariff of GFU, CNY/kwh
Ξ_{gas}	Gas price, CNY/m^3
Ξ_{sh}	Heat price, CNY/kwh
$\lambda_{\mathrm{CO_2}}$	Carbon trading price, CNY/t
ϕ	Carbon emission standard, kg/kwh
$\eta_{\mathrm{CFU}}^{\mathrm{CO_2}}, \eta_{\mathrm{GFU}}^{\mathrm{CO_2}}$	Carbon emissions per unit of fuel consumption, kg/(kwh), $kg/10^6m^3$
a, b, c	Generation parameters of CFU, -
L_{HVNG}	Natural gas low calorific value, -
$\eta_{stand-by}$	The stand-by state power ratio, -
S_{wt}	The cross-sectional area of water tank, m^2
$h^{\min}, h^{\max}$	The lower/upper pressure head limits, m
$\overline{h}$	The elevation, m
Chw	The Hazen-Williams friction factor, -
dd_{pi}	Pipe diameter, m
l_{pi}	Pipe length, m
σ_{va}	The opening ratio of valves, -
k_{pu}	The resistance coefficient of pipe, -
$\underline{P}_{\mathrm{PtG}}^{stand}$	Stand-by load of ptg, kw
$\underline{\chi}_{\mathrm{PtG}}, \overline{\chi}_{\mathrm{PtG}}$	The minimum down and up time of ptg, min

C. ABBREVIATION

PtG	Power-to-gas
IPWS	Integrated power and water system
IGDT	Information gap decision theory
HHV	Higher-heating-value
PDN	Power distribution network
WDN	Water distribution network
O&M	Operation and maintenance

I. INTRODUCTION

A. MOTIVATION AND INCITEMENT

To accelerate the decarburization of the energy network, the substitution of renewable energy for traditional generators in the power side has been considered in the energy roadmap worldwide. However, a subsequent curtailment in renewable energy should be dealt with carefully, where the wind and solar curtailment rates in China were up to 22% and 30% [1]. Power-to-gas is an optional distributed energy storage device for renewable energy, which is regarded as an promising scheme because of the large-scale and long-term storage characteristics [2]. Generally, PtG is applied in the integrated power and gas system, where its load shifting effect can be bidirectional. Playing the role as an energy converter together with gas fired units, PtG is able to increase the flexibility and reliability of the integrated system. Although there is a considerable amount of research on the application of PtG, ordinary modeling that described by empirical formula without response to the intermittency of renewable energy will greatly deviate the correct decision-making. What' more, the work that studies the role of PtG in other types of coupled networks is rare. In terms of the participation of the electrolysis process, PtG can be a critical coupling element in water networks. In this article, PtG is considered as a flexible load resource of electricity and water, and the influence of its refined reaction modeling on the operation strategy is discussed.

B. LITERATURE REVIEW AND RESEARCH GAP

This article presents accurate consumption model and running mode of PtG. The reaction model of PtG in the researches on the integrated system analysis usually lacks sufficient accuracy, while empirical coefficient can lead to significant decision-making error. There is a substantial body of work on the performance of PtG in the integrated energy system, while only a little of them established a fairly accurate theoretical model. Reference [3] made a comprehensive review on the technology and economy of PtG, which guided the subsequent studies in this field a lot. In the review, the reaction process was separated from the system analysis, which means that the refined reaction model had been rarely applied in the system scheduling model. Also, the dynamic characteristics of methanation is emphasized and it was summed up that researches generally set a stand-by state for PtG. Economic assessment of PtG is conducted with the incorporation of refined flowsheet of the PtG process design in reference [4]. However, such refined module has rarely been analyzed jointly with energy flow in system analysis or applied in energy scheduling. The reliability of energy networks incorporating PtG has been a research focus. PtG is incorporated to enhance the reliability of the integrated power-gas system (IPGS) in the references [5], [6], the general reliability indices are set and the influence on which is evaluated. In practice, however, the empirical formula used in these literatures will cause an inaccurate operation strategy of PtG plant. Then it will be followed by a significant error in reliability indices. At present, exploration on the application of refined PtG model in energy network has been carried out. An utilization of a refined model of PtG is conducted in the research on the carbon emission reduction in the IPGS in reference [7]. The power consumption is calculated considering the reaction heat and a refined hydrogen storage model is established, but it still lacks the analysis of response to the intermittency of renewable energy and the thermodynamic property can be modeled more detailed.

These works are meant to make an economic or reliable decision for PtG, while the decision will definitely be inaccurate due to an inaccurate model. For economic evaluation, the empirical model will conceal some of the power consumption, which will cause the accounting error. For operation strategy, the empirical model will conceal the mismatch between PtG device and the intermittency of renewable energy, which will cause the failure of PtG dispatching. Therefore, refined electrolytic process of PtG is modeled from the view of explicit consumption classification and by-product recovery, also, the response to the renewable energy intermittency of methanation reactor is modeled in this article.

This article establishes the coupling model of IPWS considering the coupling effect of PtG. In order to increase the reliability and flexibility, water networks has been strongly coupled with the power system. As both power load and water load, PtG can be a significant regulator in IPWS while the relevant literature is rare. Reference [8] focuses on the coupling effect of pumping devices, which is applied to stabilize the uncertainty in power and water demands. In reference [9], researchers worked to solve the storage of the surplus renewable energy by utilizing the water pumps and tanks in the water supply networks. Additionally, the coupling between water network and power system can be effective during decision-making in extreme environments. A drought situation and a power outage situation is considered in reference [10] to study the interdependencies, where a targeted generation model is built during periods of droughts. Through literature review, it can be seen that the water pump consumption can be a nonnegligible load of distribution power system. With the rapid growth of both power load and water load, a closer coupling among the water and power networks should be built. Moreover, the uncertainty brought by renewable energy will have a significant impact on the water supply, and therefore the impact should be taken into account when making scheduling strategy. To the best of our knowledge, the coupling effect of PtG on water network and power system has been rarely concerned. Thus, our article explores PtG's coupling model in IPWS.

C. CONTRIBUTION AND PAPER ORGANIZATION

The contributions of this article are:

- The model of electrolytic process of PtG is refined. The refined power consumption model during PtG process includes hydrogen production, heating and compression, in which the recovery of extra heat when heating the electrolyzer is conducted;
- The model of methanation process of PtG is refined. An idle state duration model of methanation reactor is built to illustrate the response to the intermittency of renewable energy;
- The dispatching model of IPWS considering the coupling effect of PtG is established. The power and water load of PtG are both considered, and a nonlinear mixed integer programming restrained by water pumping and power transmission constraints is carried out with convex approximation method;
- The impact of wind power uncertainty on the total revenue is evaluated with IGDT technique.

The rest of this article is organized as follows: Section II expresses the refined model of water electrolysis and methanation process. Section III presents the transmission constraints of an integrated power and water distribution network. Section VI illustrates the description of the scheduling problem as well as the application of IGDT with fluctuating wind power. Section V discusses the effectiveness of the proposed refined model and method. Finally, Section VI makes a conclusion and a future research plan.

II. MODELING OF THE PROCESS OF POWER-TO-GAS

A. THE EMPIRICAL FORMULA OF POWER-TO-GAS

For the clarity of expression and quick solution, the power-to-gas reaction is used to be formulated as:

$$f_{\mathrm{CH}_4} = P_{in} \cdot \eta_{ele} \cdot \varepsilon_{\mathrm{CH}_4} \tag{1}$$

where the output of methane is controlled by the efficiency of electrolysis process and the stoichiometric coefficient.

In our former work, the recovery of the reaction heat during methanation process is considered, and it is quantified as:

$$H_{\text{PtG,CH}_4} = \frac{P_{\text{PtG}}/\upsilon_{\text{H}_2}\rho_{\text{H}_2}}{4M_{H_2}}\frac{\Delta H_{\text{PtG}}}{3600}\eta_{\text{PtG}}^{\text{CH}_4/\text{h}} \tag{2}$$

To the best of our knowledge, no previous work on the performance of PtG in the IES has divided the input power based on the function such as hydrogen production, heating and compression, which will make an easier chance for the cost loss of compression and waste heat recovery during heating.

B. THE REFINED MODEL OF WATER ELECTROLYSIS PROCESS

PEM electrolyzer is modeled as the electrolytic section in terms of the start-up and shut-down characteristics (minute-second scale) and development stage (commercialization) [3].

In a water electrolysis system, the energy loss can be reflected by the heat losses, which can be described by comparing the cell voltage and an introduced higher-heating-value (HHV) voltage U_{HHV} [11]. The HHV voltage can be written as a function of temperature at standard pressure:

$$\text{U}_{HHV} = 1.4756 + 2.252 \cdot 10^{-4}T + 1.52 \cdot 10^{-8}T^2 \tag{3}$$

From a thermodynamic point of view, the operating voltage of a single electrolytic cell can be expressed as follows [11]:

$$\text{U}_{cell} = \frac{\text{U}_{HHV}}{\eta_E} \tag{4}$$

where U_{cell} is the cell voltage, η_E is the electrolyser efficiency.

Electrolyzers usually operates under U_{cell} and the electricity input P_{ele}, and P_{ele} is used to produce hydrogen and heat as follows [12]:

$$P_{ele} = P_{ele,\text{H}_2} + P_{ele,\text{Heat}} \tag{5}$$

$$P_{ele,\text{H}_2} = N_{stack} \cdot \text{U}_{HHV} \cdot i_{cell} \cdot S_{act} \tag{6}$$

$$P_{ele,\text{Heat}} = N_{stack} \cdot (\text{U}_{cell} - \text{U}_{HHV}) \cdot i_{cell} \cdot S_{act} \tag{7}$$

$P_{ele,\text{Heat}}$ is restrained by the thermal energy balance as:

$$P^t_{ele,\text{Heat}} - P^t_{ele,\text{Dis}} - P^t_{ele,\text{Rec}} = CT\,(t) - CT\,(t-1) \tag{8}$$

where $P^t_{ele,\text{Dis}}$ is expressed as:

$$P^t_{ele,\text{Dis}} = \frac{T\,(t) - T_{amb}}{R_{the}} \tag{9}$$

The balance constraints above also reflect the thermal dynamic behavior of the electrolyser. Moreover, it enlarges our former work on the consideration of methanation heat recovery, and $P^t_{ele,\text{Rec}}$ can be seen as another by-product of PtG.

Additionally, the consumption of the compression of the feed-in gas, CO_2, and the produced H_2 is modeled and included in the operation cost, which can be expressed as [13]:

$$P^t_{com} = \sum_{i=1}^{N_{com}} \sum_{j\in\Lambda_{gas}} Z_i \cdot R_{gas} \cdot T_i \frac{\gamma_i \cdot \eta_{com,i}}{\gamma_i - 1} \times \left[\left(\frac{p_{out,i}}{p_{in,i}}\right)^{\frac{\gamma_i-1}{\gamma_i \cdot \eta_i}} - 1\right] \cdot n_j \tag{10}$$

As we can see, the addition of the recovery of extra electrolysis heat and compression cost certainly makes the economic evaluation more convincing.

C. THE REFINED MODEL OF METHANATION PROCESS

1) THE RESPONSE MODEL OF THE METHANATION PROCESS

The fix-bed methanation reactor is usually considered as the appropriate reactor, which can be described as a cylindrical coordinate system. Therefore, two or one dimensional models indicating mass and energy balances are usually used to analyze and control the reaction. However, such micro and dynamic analysis may be inappropriate for the decision-making of the large scale energy system. It can lead to the phenomenon that refined reaction flow of PtG is rarely analyzed in energy dispatching model researches. On the one hand, the methanation process is significantly influenced by temperature, pressure, composition and reactor parameters, which makes it difficult to find a general application scenario. On the other hand, the time scale of the transient reaction (100∼400s) is far shorter than that of the integrated energy system (15min∼hours) [14], and the process control of methanation is outside this paper's scope.

However, the ordinary empirical formula mainly has the following two shortcomings: 1) The compression consumption of feed gas are rarely considered, which is necessary for the generation scheduling and running economy evaluation; 2) The start-up and shut down of methanation reactor will significantly influence the operation strategy, especially considering the intermittency of wind power, so it should be modeled appropriately.

To match the intermittent output of renewable energy, the methanation reaction has to achieve high-efficiency conversion in a completely dynamic mode of operation, so it requires a further study in the restart performance. Generally, the initial start-up of methanation process requires external heating. However, after a succession of gas shut down and reinjection, the process could restart spontaneously. Based on the technology of a multi-tubular wall-cooled fixed-bed reactor introduced in reference [15] and the study in reference [16], it turns out that the restart speed varies linearly with the idle state duration and the temperature decrease. The function can be expressed as follows.

$$1/\tau_{res} = A + B \cdot \Pi_{idle} \tag{11}$$

where τ_{res} is the restart time, Π_{idle} is the idle state duration, A,B are constant coefficients related to reactor's structure.

For linearization, Taylor's Formula is used to linearize the fraction term, $1/\tau_{res}$. According to reference [16], we chose 500s as the Taylor expansion point, and terms higher than quadratic are removed as their contribution is too small. Then Eq.(11) is transferred to:

$$\frac{1}{500} - \frac{1}{500^2} \cdot (\tau_{res} - 500) = A + B \cdot \Pi_{idle} \tag{12}$$

It is assumed that the state of electrolyzer is consistent with the methanation reactor, and then the electrolyzer's start-up time and idle duration should be restrained to:

$$\frac{1}{500} \cdot u_{start,t} - \frac{1}{500^2} \cdot \left(\tau_{res,t} - 500 \cdot u_{start,t}\right) = A \cdot u_{start,t} + B \cdot \Pi_{idle} \tag{13}$$

$$0 \leq \tau_{res,t} \leq u_{idle,t} \cdot M \tag{14}$$

$$0 \leq \Pi_{idle,t} \leq u_{idle,t} \cdot M \tag{15}$$

$$-1 + \sum_{t=1}^{T} u_{idle,t} \leq \frac{1}{\mathrm{SI}} \cdot \left(\tau_{res,t} + \Pi_{idle,t}\right) \leq 1 + \sum_{t=1}^{T} u_{idle,t} \tag{16}$$

$$u_{on,t} \cdot \underline{P}_{\mathrm{PtG}} + u_{stand,t} \cdot P_{\mathrm{PtG}}^{stand} + u_{start,t} \cdot P_{\mathrm{PtG}}^{start} \leq P_{\mathrm{PtG},t} \leq \left(u_{on,t} + u_{stand,t}\right) \cdot M + u_{start,t} \cdot P_{\mathrm{PtG}}^{start} \tag{17}$$

$$u_{idle,t} + u_{on,t} + u_{stand,t} = 1 \tag{18}$$

$$u_{idle,t} + \sum_{\chi=t+1}^{\min\left(T,t+\underline{\chi}_{\mathrm{PtG}}\right)} \left(u_{on,t} + u_{stand,t}\right) \leq 1 \tag{19}$$

$$\left(u_{on,t} + u_{stand,t}\right) + \sum_{\chi=t+1}^{\min\left(T,t+\overline{\chi}_{\mathrm{PtG}}\right)} u_{idle,t} \leq 1 \tag{20}$$

where SI is the load sampling interval, 5 min, which is decided according to the average start-up time in reference[16]. Eq.(13-16) illustrate the length limitation of idle phase; Eq.(17-18) restrain the operation state of PtG; Eq.(19-20) restrain the minimum length of on/off state of PtG.

2) THE CLASSIFICATION OF THE INTERMITTENT PERIOD SCENARIO

Beside the latter simulation demonstration, we make a theoretical analysis on the choice of PtG's optimal operation strategy between the scheme with idle phase and the scheme keeping a stand-by load. Before decision-making, we know that: 1) the start-up and shut-down duration is included in the intermittent time of PtG; 2) the idle duration should be separated from the time that maintains a stand-by load. On these premise, the following scenarios are divided:

(1) As shown in Fig.1(a), the upper limit of the sum of the start-up time and idle state duration is shorter than the intermittent period. ($Max\left(\Delta T_{start-up} + \Delta T_{idle}\right) < \Delta T_{\mathrm{int}}$)

In this scenario, the reactor will operate in a circular mode that starts with a stand-by load, and then there will be an idle phase. Finally, the reactor will restart. For the concern of cost saving, the idle period should be as long as possible.

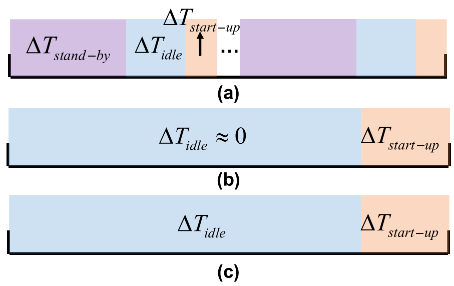

FIGURE 1. Diagram of PtG's operation state.

Take one cycle for a case, the power consumption during one cycle is:

$$\sum_{t\in\underline{T}_{stand-by}} P_{stand-by} + \sum_{t\in T_{start-up}} P_{\mathrm{PtG},start} = \eta_{stand-by}\overline{P}_{\mathrm{PtG}} \cdot \Delta\underline{T}_{stand-by} + \overline{P}_{\mathrm{PtG}} \cdot \Delta T_{start-up} \tag{21}$$

While the power consumption without considering the idle phase is:

$$\sum_{t\in T_{cycle}} P_{stand-by} = \eta_{stand-by}\overline{P}_{\mathrm{PtG}} \cdot \Delta T_{cycle} \tag{22}$$

Under this circumstance, the introduction of the idle phase will provide a significantly cost-saving operation scheme.

(2) As shown in Fig.1(b), the lower limit of the sum of the start-up time and idle state duration is longer than the intermittent period. ($Min\left(\Delta T_{start-up} + \Delta T_{idle}\right) > \Delta T_{\mathrm{int}}$)

In this scenario, even the shortest idle duration will cover the intermittent period of RE (when $\Pi_{idle} \approx 0$). The reactor will keep in stand-by state in the circumstance.

(3) As shown in Fig.1(c), the intermittent period is between the value described in the former two scenarios.

$$(Min\left(\Delta T_{start-up} + \Delta T_{idle}\right) \leq \Delta T_{\mathrm{int}} \leq Max\left(\Delta T_{start-up} + \Delta T_{idle}\right))$$

In this scenario, the reactor can keep in idle phase without a stand-by load. Then, the consumption under idle mode is:

$$\begin{cases} \sum_{t\in T_{start-up}} P_{\mathrm{PtG},start} = \overline{P}_{\mathrm{PtG}} \cdot \Delta T_{start-up} \\ \Delta T_{idle} + \Delta T_{start-up} = \Delta\underline{T}_{stand-by} \end{cases} \tag{23}$$

While the consumption without considering the idle phase is:

$$\sum_{t\in\underline{T}_{stand-by}} P_{stand-by} = \eta_{stand-by}\overline{P}_{\mathrm{PtG}} \cdot \Delta\underline{T}_{stand-by} \tag{24}$$

Under this circumstance, we can easily attain that a balance between stand-by mode and idle mode will be achieved if the following equation holds:

$$\eta_{stand-by}\overline{P}_{\mathrm{PtG}} \cdot \Delta T_{stand-by}^{0} = \eta_{stand-by}\overline{P}_{\mathrm{PtG}} \cdot \Delta T_{stand-by}^{1} + \overline{P}_{\mathrm{PtG}} \cdot \Delta T_{start-up}^{1} \tag{25}$$

where the duration under scheme S0 and S1 should be constrained as:

$$\Delta T^{0}_{stand-by} = \Delta T^{1}_{stand-by} + \Delta T^{1}_{idle} + \Delta T^{1}_{start-up} \quad (26)$$

To sum up, the operating strategy is made optimally depending on the length of the intermittent period of RE.

III. MODLING OF AN INTEGRATED POWER-WATER SYSTEM

A. WATER DISTRIBUTION NETWORK MODEL

Two assumptions are given as follows:

1) The on/off statuses of supply pumps are determined before scheduling;

2) The direction of pipe flow does not change during scheduling.

These assumptions can be commonly seen in the works (see [17], [18], [19]). In this paper, it is set that water is supplied by water tanks. To be specific, water is pumped into the elevated tanks so that tanks can release the pressurized water with the regulation by valves in the pipes. Therefore, the water distribution process can be described by the node hydraulic head and the pipe flow rate, which is divided into node, pipe and path constraints as follows:

1) NODE CONSTRAINTS

$$d_{i,t} = \sum_{ij\in P_i} q_{ij,t} - \sum_{ki\in P_i} q_{ki,t} \quad (27)$$

$$H^{t}_{i,out} = H^{t-1}_{i,out} + \frac{\Delta T}{S_{wt}} d_{i,t} \quad (28)$$

$$h^{\min}_i + \bar{h}_i \le H^{t}_{i,out} \le h^{\max}_i + \bar{h}_i \quad (29)$$

where Eq.(27) gives the relation of water load and pipe flow; Eq.(28) shows how water tanks work at the load nodes; Eq.(29) gives the hydraulic head constraints of water tanks[8].

2) PIPE CONSTRAINTS

Head losses in valves, pipes and pumping heads of the pump stations are inevitable and should be considered in water distribution, which can be expressed as follows:

$$h_{pi} = 10.708 \cdot q^2_{pi} \mathrm{Chw}^{-1.852} dd_{pi}{}^{-4.87} l_{pi} \quad (30)$$

$$h_{va} = 10^{-6} q_{pi,va\in pi}{}^{2} \sigma_{va}{}^{-2} \quad (31)$$

where Eq.(30-31) give the losses in pipes and valves. Chw is the Hazen-Williams friction factor; d_{pi}, l_{pi} are the pipe diameter and length respectively; σ_{va} is the opening ratio of valves.

Each consumer node is linked with a resource node through a path, where the pumping heads of the pump stations in the paths are expressed as:

$$h_{pu,t} = k_{pu} \cdot \left(q^{pu\in pi}_{pi,t}\right)^n \quad (32)$$

Through the introduction of a constant, δ_{pu}, with units of kW/CMH·m, the power consumption of the pump station can be expressed as:

$$P_{pu,t} = -\delta_{pu} \cdot h_{pu,t} \cdot q^{pu\in pi}_{pi,t} \quad (33)$$

In this article, the Darcy-Weisbach formula in which $n = 2$ is used to describe the pumping head:

$$h_{pu,t} \ge k_{pu} \cdot \left(q^{pu\in pi}_{pi,t}\right)^2 \quad (34)$$

The quadratic term of Eq.(34) is neglected as its contribution is small [20], and then the pumping head is formulated as:

$$h_{pu,t} = -\left(\vartheta_{pu,0} + \vartheta_{pu,1} q_{pi,t}\right) \quad (35)$$

By applying the convex approximation approach from reference [20], the power consumption function, Eq.(33), can be relaxed with its convex hull:

$$\begin{aligned} P_{pu,t} &\ge -\delta_{pu} \cdot h_{pu,t} \cdot q^{pu\in pi}_{pi,t} \\ P_{pu,t} &\le -\delta_{pu} \cdot \left(\varpi_{pu,0} + \varpi_{pu,1} q_{pu,t}\right) \end{aligned} \quad (36)$$

where $\varpi_{pu,0}$ and $\varpi_{pu,1}$ provide the upper bound for the convex hull.

3) PATH CONSTRAINTS

A water system can be described as a graph ⟨N, P⟩, where N denotes nodes and P denotes paths. The cyclic matrices, L_k, related to pump stations and valves can be expressed as:

$$\mathrm{L}_k = \mathrm{L}_a \mathrm{P}^T_k, \quad k = pu,\ va \quad (37)$$

where P_k describes the placement of pump stations and valves on pipe ij by:

$$(\mathrm{P}_k)_{ij} = \begin{cases} 1, & k \in ij \\ 0, & k \notin ij \end{cases} \quad (38)$$

For each specific path P, the Kirchoff's second law should be followed as:

$$\mathrm{L}_{pu} h_{pu} - \mathrm{L}_{pi} h_{pi} - \mathrm{L}_{va} h_{va} = \varepsilon_{pa} \quad (39)$$

where ε_{pa} is the head difference between the ends of the path, and $\varepsilon_{pa} = 0$ when the path is a loop.

B. POWER DISTRIBUTION NETWORK MODEL

It is assumed that the voltage level of IPWS is 12.66 kV, and the physical constriction of PDN is expressed as follows.

$$\begin{aligned} &P^{CFU}_{i,t} + P^{GFU}_{i,t} + P^{WT}_{i,t} + \sum_{k\in i,k\ne i} \left(P^{\text{line}}_{ki,t} - I_{ki,t} r_{ki}\right) \\ &= P^{PtG}_{i,t} + \alpha_{\mathrm{Le},i} P^{\text{load}}_{i,t} + \sum_{j\in i,j\ne i} P^{\text{line}}_{ij,t} \end{aligned} \quad (40)$$

$$\begin{aligned} &\mathrm{Q}^{CFU}_{i,t} + \sum_{k\in i} \left(Q^{\text{line}}_{ki} - I_{ki,t} x_{ki}\right) \\ &= Q^{\text{load}}_{i,t} + \sum_{j\in i,j\ne i} Q^{\text{line}}_{ij,t} \end{aligned} \quad (41)$$

$$U_{i,t} - U_{j.t} = -2\left(P^{\text{line}}_{ji,t} r_{ji} + Q^{\text{line}}_{ji,t} x_{ji}\right) + I_{ji,t}\left(r^2_{ji} + x^2_{ji}\right) \quad (42)$$

$$\underline{U_i} \leq U_i \leq \overline{U_i},\ \underline{I_{ij}} \leq I_{ij} \leq \overline{I_{ij}} \tag{43}$$

$$U_{i,t} I_{ij,t}^{\text{line}} = \left(P_{ij,t}^{\text{line}}\right)^2 + \left(Q_{ij,t}^{\text{line}}\right)^2 \tag{44}$$

where Eq.(40-41) represent active and reactive power balance; Eq.(42-43) represent constraints of voltage and current; Eq.(44) represents transmission constraint.

IV. DAY-AHEAD GENERATION SCHEDULING MODEL OF IPWS

A. OBJECTIVE FUNCTION

Since it is validated that PtG is unprofitable when running individually under today's price environment in our former work [21], PtG is seen as a member of the union consisting of a distribution power utility and a distribution water utility. In this condition, a decision is made to minimize the total operational cost of the integrated power-water system. For the cost, the operation cost of the units, the penalty of wind power abandonment and the carbon dioxide cost are considered. For the profit, the distribution revenue of power distribution network (PDN) and water distribution network (WDN), the carbon trading income and the by-product benefit of PtG are considered. The objective function is expressed as follows:

$$\begin{aligned}
&Max\ F_R \\
&\quad = R_{op} - C_{op} \\
&\quad = \sum_{t=1}^{T} \left(\begin{aligned} &\Xi_{\text{fe-WT}} \cdot P_{\text{WT},t} + \Xi_{\text{fe-CFU}} \cdot P_{\text{CFU},t} \\ &+ \Xi_{\text{fe-GFU}} \cdot P_{\text{GFU},t} + \Xi_{tran,PDN} \\ &\times \left(P_{\text{WT},t} + \sum_{\text{CFU} \in \Omega_{\text{U}}} P_{\text{CFU},t} + \sum_{\text{GFU} \in \Omega_{\text{U}}} P_{\text{GFU},t} \right) \\ &+ \lambda_{\text{CO}_2} \left(D_{\text{CFU},t} + D_{\text{GFU},t} - E_{\text{CFU},t} \right. \\ &\left. + E_{\text{GFU},t} \right) + \Xi_{\text{gas}} ff_{\text{PtG},t} + \Xi_{sh} \text{H}_{\text{PtG},t} \\ &+ \Xi_{tran,WDN} \sum_{i=1}^{N} d_{i,t} \end{aligned} \right) \\
&\quad - \sum_{t=1}^{T} \left(\begin{aligned} &c_{\text{CFU}} \sum_{\text{CFU} \in \Omega_{\text{U}}} P_{\text{CFU},t} \\ &+ c_{\text{GFU}} \sum_{\text{GFU} \in \Omega_{\text{U}}} P_{\text{GFU},t} \\ &+ c_{\text{WT}} \left(\widetilde{P}_{\text{WT},t} - P_{\text{WT},t} \right) \\ &+ c_{\text{CO}_2} \mu_{\text{PtG,CO}_2} P_{\text{PtG},ele} \end{aligned} \right) \\
&s.t.\ (3) - (10), (12) - (20), (27) - (31), \\
&\quad (35) - (44)
\end{aligned} \tag{45}$$

The economic evaluation of integrated energy system with high proportion of renewable energy is increasingly involving carbon trading issues [22], [23]. Since carbon trading is an essential factor in measuring the benefits of Power-to-X technique because of the carbon capture before gas-intake, it is included in the objective function represented by $\lambda_{\text{CO}_2} (D - E)$ in Eq.(45), which can be illustrated in detail as follows:

$$D_G = \phi \sum_{G \in \{\text{CFU,GFU}\}} \sum_{t=1}^{T} P_{\text{G},t}^{f}$$

$$E_{\text{CFU}} = \sum_{t=1}^{T} \eta_{\text{CFU}}^{\text{CO}_2} \left(a_{\text{CFU}} + b_{\text{CFU}} P_{\text{CFU},t} + c_{\text{CFU}} P_{\text{CFU},t}^2 \right)$$

$$E_{\text{GFU}} = \sum_{t=1}^{T} \eta_{\text{GFU}}^{\text{CO}_2} P_{\text{GFU},t} / \left(\eta_{\text{GT}} L_{\text{HVNG}} \right) \tag{46}$$

The high construction and O&M cost has hindered the commercialization of PtG, and the integrated power and water system will provide a profitable scheme.

B. IGDT-BASED GENERATION SCHEDULING MODEL CONSIDERING WIND POWER UNCERTAINTY

Generation forecast errors in renewable energy always exist. Enlightened by the approaches in the literatures, IGDT technique can be effective to solve an risk-assess decision making problem. The theory describes an uncertain model from both the favorable and adverse perspective, to be specific, the theory can be applied to maximize the robustness or revenue against uncertainty [24]. Using the envelop-bound model of IGDT, the uncertain parameters can be modeled as follows.

$$B(\alpha, b_0) = \{b : b = (1 + \alpha) b_0\} \tag{47}$$

where b is the uncertain variable, b_0 is the nominal value, and α is the extent of the fluctuation.

In this article, wind power uncertainty is the uncertainty in the model. If the worst scenario is considered, the greatest variation should be incorporated as

$$(1 - \alpha) \widetilde{P}_{\text{WT},t} \tag{48}$$

where α represents the fluctuation of wind power. $P_{\text{WT},i}^{0}$ denotes the forecasted wind power output.

Generally, a discounted objective value should be set by the operator before IGDT technique is applied. In this case, the IPWS union operator predicts the target revenue with a discount coefficient of the revenue under the baseline case, β. Therefore, the IGDT-based robust dispatching considering uncertainty is modeled as follows:

$$\begin{aligned}
&\text{Obj.}\ \max_{\beta} \left\{ \min_{P_{wt} \in \Theta} F_R \left(\Theta, P_{\text{WT},t} \right) \geq (1 - \beta) F_R^{base} \right\} \\
&s.t.\ P_{\text{WT},t} \geq (1 - \alpha) \widetilde{P}_{\text{WT}} \\
&\qquad (3) - (10), (12) - (20), (27) - (31), (35) - (44)
\end{aligned} \tag{49}$$

The objective function is to maximize the dispatching revenue, while the dispatching revenue is guaranteed to be equal to or higher than a discount of the revenue under the deterministic scenario. Meanwhile, the fluctuation range of renewable energy is limited to be no wider than a discount with α.

V. CASE STUDIES

A. CONFIGURATION AND PARAMETER SETTING OF IPWS

In this article, a topology coupled by a modified IEEE 33-node power distribution system and 9-node water distribution network in reference [25] is used, which is shown in

Fig.2 Operation parameters of the generators, cost parameters are shown in [26].

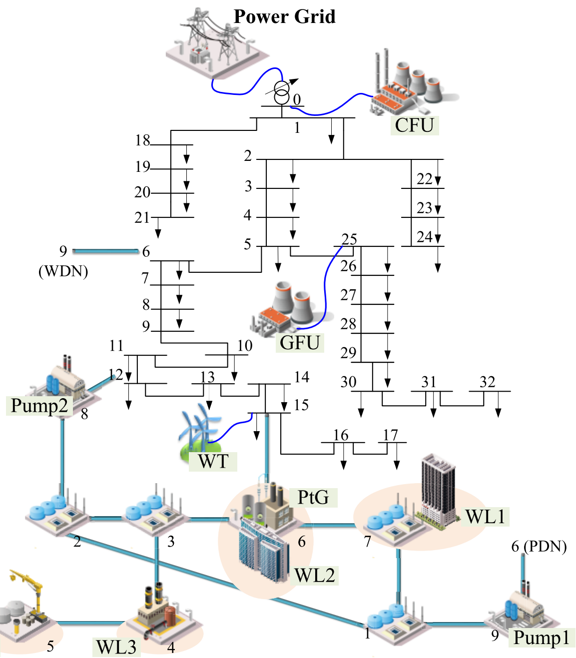

FIGURE 2. Constructure of integrated power and water system.

All tests are run on an Intel(R) Core(TM) i7-7700HQ CPU @2.80GHz personal computer with 8GB RAM. Programs are coded on Matlab Yalmip and solved with solver CPLEX.

B. THE IMPACT OF THE APPLICATION OF REFINED PTG MODEL

1) THE CONSIDERATION OF REFINED ELECTROLYSIS PROCESS

In this article, a refined electrolysis process is modeled. To be specific, the input power is divided into the power for hydrogen production, electrolyser heating and compression of the feed gas. Compared with the traditional empirical formula where the production is mainly decided by electrolysis efficiency, the proposed model has the following advantages:

(1) Researchers can be more familiar with the relation between electrolysis output and input;
(2) The easily neglected energy, the extra heat during electrolysis heating, can be recovered as a by-product;
(3) The consumption of feed gas compression before methanation can significantly increase the O&M cost, which should not be neglected.

Simulation results present the comparison between the traditional and refined model.

Fig.3 shows the extra heat which is recoverable based on the theoretical conditions. It is worth mentioning that only theoretical recovery amount is illustrated, and a further research and development on the device is necessary. We can see from Fig.3 that a daily recovery amount can be up to 1104.9 kWh reaching 26.6% of the total consumption of electrolyzer, and it would be considerable if the PtG plant gets larger.

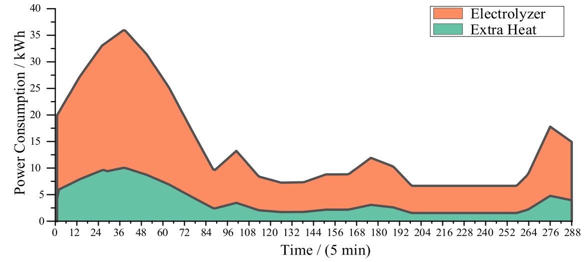

FIGURE 3. Total recoverable heat during electrolysis heating.

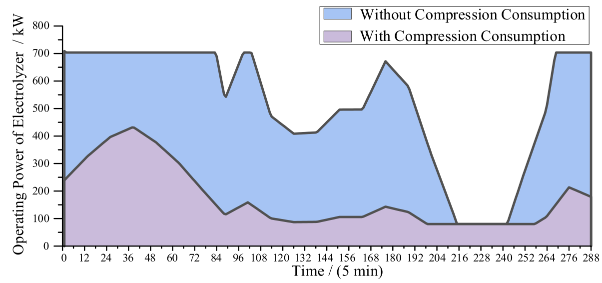

FIGURE 4. Comparison between before and after the allowance for consumption of compression.

From the comparison between before and after the allowance for consumption of compression, it can be found that PtG will operate at its upper point more frequently without the consideration, where the total consumption of the water electrolysis is lifted 197.8% and the growth is 61.9% for the consumption of PtG. In other words, the ignorance of compression will influence the scheduling model of PtG greatly. What's worse, PtG is supposed not to perform at a high point during day time (7.a.m∼19.p.m) for the sake of low wind power, while the maximum operation point is still reached when the compression is neglected.

2) THE CONSIDERATION OF REFINED METHANATION PROCESS

In this article, the start-up time and idle state duration is considered, which replaces the traditional model where PtG does not response to the intermittency of renewable energy or keeps operating over a certain stand-by load.

Based on the classification in Section II, the impact of refined methanation process is demonstrated. The study is conducted on the following basis:

(1) An almost 100%-RE-penetration power system is built, and PtG is set as the only power load;
(2) The fixed-bed reactor characteristic in Fig.5 from in literature [16] is applied so that the upper and lower limit of the sum of the start-up time and idle state duration is fixed.
(3) The stand-by load is $0.1\overline{P}_{\mathrm{PtG}}$, while the start-up power is $\overline{P}_{\mathrm{PtG}}$.

(4) Referring to the existing technique of fixed-bed reactor, we leave out the second classification, which is $Min\left(\Delta T_{start-up} + \Delta T_{idle}\right) > \Delta T_{\text{int}}$, considering that the minimum shut-down duration lasts longer than $Min\left(\Delta T_{start-up} + \Delta T_{idle}\right)$.
(5) The objective is to minimize the operation cost of wind power and PtG.

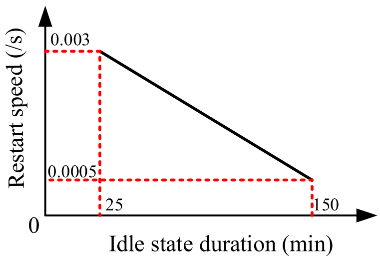

FIGURE 5. Characteristics of idle phase.

In the scenario, the wind power during daytime, 7:00 a.m.∼16:00 p.m., is set as 0. To illustrate the decision making in a short intermittent interval, we assume that a breakdown occurs from 20:00 p.m. to 22:00 p.m. The minimum and maximum of on/off duration are both set as 1 hour.

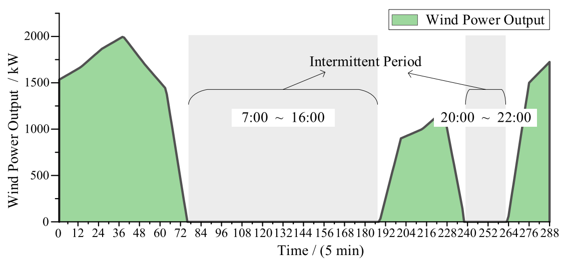

FIGURE 6. Parameter of wind output.

As shown obviously in Fig.6, an intermittent operation strategy is implemented by the water electrolysis. Beside the intermittent duration, the water electrolysis follows the curve of wind power. When it comes to the intermittent duration, the results demonstrate our former analysis: 1) the stand-by and idle phase will be under cyclic switching when ΔT_{int} is much longer than $\Delta T_{idle} + \Delta T_{start}$; 2) the idle and restart phase will fill ΔT_{int} when ΔT_{int} is between the minimum and maximum of $\Delta T_{idle} + \Delta T_{start}$. These two scenarios should certainly be restrained by constraints Eq.(13∼20). Compared with the scheme maintaining a stand-by load during the intermittent period that consumes 920.0 kWh ([7:00,16:00] and [20:00,22:00]), the water electrolysis with the refined methanation process consumes 718.3 kWh. Therefore, the power consumption of the water electrolysis is reduced significantly by 21.9%.

C. IGDT BASED DAY-AHEAD SCHEDULING STRATEGY

In this case, the IGDT technique is applied in the IPWS decision making to study the union revenue variation when the output of RE is uncertain.

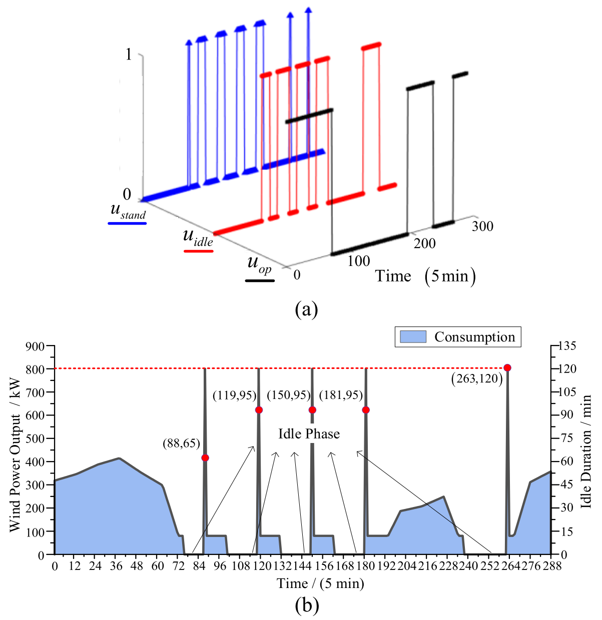

FIGURE 7. Operation strategy of PtG applying a refined methanation process:(a) PtG's operation state. (b) electrolyzer's consumption.

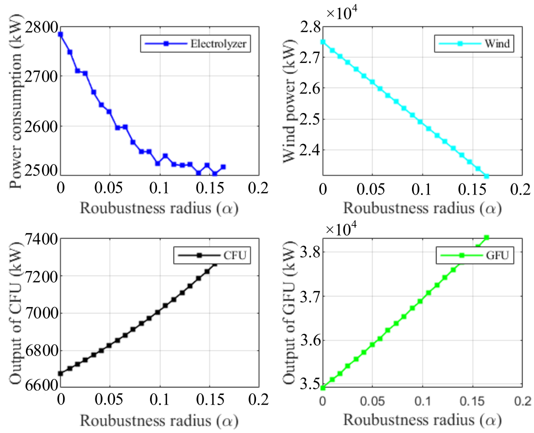

FIGURE 8. Solution of the units output using an uncertain model based on IGDT technique.

Fig.7 illustrates the influence of the wind power fluctuation on the units output and PtG consumption. The decline of PtG's consumption shows a trend from fast to slow. The output of CFU, in turn, increases slowly and then rapidly. Meanwhile, the trend in wind power and GFU's output is almost linear. Therefore, the curves says that there is a direct competition between wind power and GFU. Moreover, the contribution of PtG to the union revenue becomes prominent as the total PND revenue comes to a low level.

As is illustrated in Eq.(48), the case study aims at finding the largest robustness factor so that the IPWS revenue will reach the given critical value. To be specific, a variation with $1-\alpha$ in the output of RE is performed, and then the lower limit of IPWS revenue is studied to reflect the guarantee against the intermittency of renewable energy. We can easily see

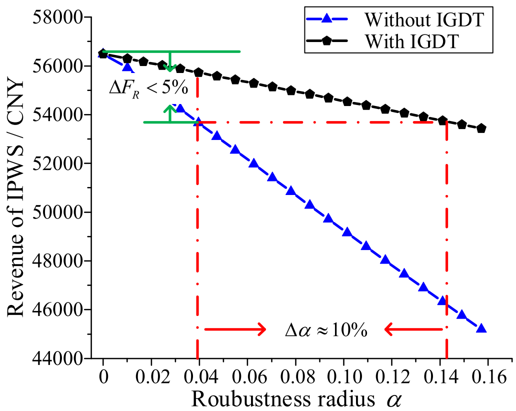

FIGURE 9. Comparison between the strategy using IGDT technique and without IGDT in terms of the revenue of IPWS.

from Fig.8 that the decline in the revenue of the IGDT-based solution is more slower than that of the without-IGDT solution, which shows that the robustness of IGDT-based IPWS decision making considering the intermittency of renewable energy. Based on the comparison in Fig.8, we can assume that the IPWS operator made a conservative prediction for decline of the union revenue to be no more than 5%, which is 53664.4 CNY. In this condition, the maximum variation of wind power that the operator can tolerate should be no higher than 4.0%. While the variation can reach more than 14.0% when the IGDT technique is applied, that is, the IGDT-based decision-making model will be a wise choice when the system operator is a risk-seeker.

VI. CONCLUSION

With the increasingly coupling of energy networks, exploring the regulation effect of coupling equipment is of great significance. Therefore, this article contributes a refined power-to-gas model for the application in an integrated power and water system. The traditional empirical model is improved from the view of refining the water electrolysis and methanation process respectively. The effectiveness is discussed through the demonstration case of an IGDT-based scheduling scheme. The results show that the recoverable extra heat during electrolytic process can reach 26.6% of the total power consumption of electrolyzer, and the ignorance of feed-in gas compression can cause a growth of power consumption by 61.9% for power-to-gas. Also, the proposed response model of power-to-gas is proved to be able to react to the renewable energy intermittency appropriately, as well as to save the power consumption significantly by 21.9%. The enlargement effect of uncertain wind power tolerance with IGDT is also verified. However, the study did not involve a complete industrial chain of power-to-gas. In order to realize the construction in the integrated energy system, the future work will focus on exploring the potential of power-to-gas: 1) A comprehensive economy and security evaluation in the power-water-gas network will be conducted with the refined power-to-gas process; 2) Multiple uncertainties will be considered in the decision-making process, on which the effectiveness of IGDT technique will be analyzed.

REFERENCES

[1] M. Chen, Z. Shen, L. Wang, and G. Zhang, "Intelligent energy scheduling in renewable integrated microgrid with bidirectional electricity-to-hydrogen conversion," *IEEE Trans. Netw. Sci. Eng.*, vol. 9, no. 4, pp. 2212–2223, Jul. 2022, doi: 10.1109/TNSE.2022.3158988.

[2] X. Zhang, C. Bauer, C. L. Mutel, and K. Volkart, "Life cycle assessment of power-to-gas: Approaches, system variations and their environmental implications," *Appl. Energy*, vol. 190, pp. 326–338, Mar. 2017.

[3] M. Götz, J. Lefebvre, F. Mörs, A. M. Koch, F. Graf, and S. Bajohr, "Renewable power-to-gas: A technological and economic review," *Renew. Energy*, vol. 85, pp. 1371–1390, Jan. 2016.

[4] F. Kirchbacher, M. Miltner, W. Wukovits, and M. Harasek, "Economic assessment of membrane-based power-to-gas processes for the European biogas market," *Renew. Sustain. Energy Rev.*, vol. 112, pp. 338–352, Sep. 2019.

[5] Z. Zeng, T. Ding, Y. Xu, Y. Yang, and Z. Dong, "Reliability evaluation for integrated power-gas systems with power-to-gas and gas storages," *IEEE Trans. Power Syst.*, vol. 35, no. 1, pp. 571–583, Jan. 2020.

[6] M. Bao, Y. Ding, C. Shao, Y. Yang, and P. Wang, "Nodal reliability evaluation of interdependent gas and power systems considering cascading effects," *IEEE Trans. Smart Grid*, vol. 11, no. 5, pp. 4090–4104, Sep. 2020.

[7] Z. Cao, J. Wang, Q. Zhao, Y. Han, and Y. Li, "Decarbonization scheduling strategy optimization for electricity-gas system considering electric vehicles and refined operation model of power-to-gas," *IEEE Access*, vol. 9, pp. 2169–3536, 2021.

[8] A. Stuhlmacher and J. L. Mathieu, "Chance-constrained water pumping to manage water and power demand uncertainty in distribution networks," *Proc. IEEE*, vol. 108, no. 9, pp. 1640–1655, Sep. 2020.

[9] D. Fooladivanda, A. D. Dominguez-Garcia, and P. W. Sauer, "Utilization of water supply networks for harvesting renewable energy," *IEEE Trans. Control Netw. Syst.*, vol. 6, no. 2, pp. 763–774, Jun. 2019.

[10] S. Zuloaga and V. Vittal, "Integrated electric power/water distribution system modeling and control under extreme mega drought scenarios," *IEEE Trans. Power Syst.*, vol. 36, no. 1, pp. 474–484, Jan. 2021.

[11] J. Koponen, "Review of water electrolysis technologies and design of renewable hydrogen production systems," M.S. thesis, Dept. Energy Syst., Lappeenranta Univ. Technol., Lappeenranta, Finland, 2015.

[12] Y. Cheng, M. Liu, H. Chen, and Z. Yang, "Optimization of multi-carrier energy system based on new operation mechanism modelling of power-to-gas integrated with CO_2-based electrothermal energy storage," *Energy*, vol. 216, Feb. 2021, Art. no. 119269.

[13] F. Salomone, E. Giglio, D. Ferrero, M. Santarelli, R. Pirone, and S. Bensaid, "Techno-economic modelling of a power-to-gas system based on SOEC electrolysis and CO_2 methanation in a RES-based electric grid," *Chem. Eng. J.*, vol. 377, Dec. 2019, Art. no. 120233.

[14] J. Bremer, K. H. G. Rätze, and K. Sundmacher, "CO_2 methanation: Optimal start-up control of a fixed-bed reactor for power-to-gas applications," *AIChE J.*, vol. 63, no. 1, pp. 23–31, Jan. 2018.

[15] S. Rönsch, J. Schneider, S. Matthischke, M. Schlüter, M. Götz, J. Lefebvre, P. Prabhakaran, and S. Bajohr, "Review on methanation—From fundamentals to current projects," *Fuel*, vol. 166, pp. 276–296, Feb. 2016.

[16] A. Fache, F. Marias, V. Guerré, and S. Palmade, "Intermittent operation of fixed-bed methanation reactors: A simple relation between start-up time and idle state duration," *Waste Biomass Valorization*, vol. 11, no. 2, pp. 447–463, Feb. 2020.

[17] D. Fooladivanda and J. A. Taylor, "Energy-optimal pump scheduling and water flow," *IEEE Trans. Control Netw. Syst.*, vol. 5, no. 3, pp. 1016–1026, Sep. 2018.

[18] A. S. Zamzam, E. Dall'Anese, C. Zhao, J. A. Taylor, and N. D. Sidiropoulos, "Optimal water–power flow-problem: Formulation and distributed optimal solution," *IEEE Trans. Control Netw. Syst.*, vol. 6, no. 1, pp. 37–47, Mar. 2019.

[19] K. Oikonomou and M. Parvania, "Optimal coordination of water distribution energy flexibility with power systems operation," *IEEE Trans. Smart Grid*, vol. 10, no. 1, pp. 1101–1110, Jan. 2019.

[20] Q. Li, S. Yu, A. S. Al-Sumaiti, and K. Turitsyn, "Micro water-energy nexus: Optimal demand-side management and quasi-convex hull relaxation," *IEEE Trans. Control Netw. Syst.*, vol. 6, no. 4, pp. 1313–1322, Dec. 2019.

[21] D. Li, C. Gao, T. Chen, X. Guo, and S. Han, "Planning strategies of power-to-gas based on cooperative game and symbiosis cooperation," *Appl. Energy*, vol. 288, Apr. 2021, Art. no. 116639.
[22] Y. Wang, Z. Li, F. Wen, I. Palu, Y. Sun, L. Zhang, and M. Gao, "Energy management for an integrated energy system with data centers considering carbon trading," in *Proc. IEEE Power Energy Soc. Gen. Meeting (PESGM)*, Aug. 2020, pp. 1–5.
[23] D. Yadav, S. Mekhilef, B. Singh, and M. Rawa, "Carbon trading analysis and impacts on economy in market-to-market coordination with higher PV penetration," *IEEE Trans. Ind. Appl.*, vol. 57, no. 6, pp. 5582–5592, Nov. 2021.
[24] M. Song, R. R. Nejad, and W. Sun, "Robust distribution system load restoration with time-dependent cold load pickup," *IEEE Trans. Power Syst.*, vol. 36, no. 4, pp. 3204–3215, Jul. 2021.
[25] D. Cohen, U. Shamir, and G. Sinai, "Optimal operation of multi-quality water supply systems-II: The Q-H model," *Eng. Optim.*, vol. 32, no. 6, pp. 687–719, Jan. 2000.
[26] D. Li. *Integrated Power and Water System*. Accessed: Apr. 29, 2022. [Online]. Available: https://figshare.com/s/9e92944ea339d37b2392

DONGSEN LI received the bachelor's degree in electrical and electronic engineering from the Hefei University of Technology, Hefei, China, in 2017. He is currently pursuing the Ph.D. degree in electric power system engineering with Southeast University, Nanjing, China. His research interest includes integrated energy system simulation and optimization.

CIWEI GAO (Senior Member, IEEE) received the bachelor's degree in electrical engineering from North China Electric Power University, Baoding, China, in 1999, the master's degree in electrical engineering from Wuhan University, Wuhan, China, in 2002, and the Ph.D. degree in electric power system engineering from Shanghai Jiao Tong University, Shanghai, China, in 2006. He is currently a Member of the Forum of Chinese Power Development and Reform (30 members) and the Director of the Electric Power Economic Technology Research Institute, Southeast University. His main research interests include integrated energy system planning and demand response in power systems. He received the Jiangsu Provincial Science and Technology Award (the second prize), in 2020.

TAO CHEN (Member, IEEE) received the B.S. degree from Anhui University, Hefei, China, in 2012, the M.S. degree from the Tampere University of Technology, Tampere, Finland, in 2014, and the Ph.D. degree from the University of Michigan–Dearborn, Dearborn, MI, USA, in 2018, all in electrical engineering. He was a Postdoc with Virginia Tech, from 2018 to 2019. He is currently a Lecturer in electricity market and machine learning with the School of Electrical Engineering, Southeast University, Nanjing, China. His research interests include power systems, demand side management, and electricity market.

JUAN ZUO received the B.Eng. degree in mechanical engineering and automation from the Nanjing University of Aeronautics and Astronautics, Nanjing, China, in 2004, and the master's degree in electric power system and automation from the State Grid Electric Power Research Institute, Nanjing, in 2010. She is now working in State Grid Shanghai Interconnection Research Institute Co., Ltd., and she is an on-the-job Ph.d. in Shanghai Jiaotong University. Her research interests include virtual power plant scheduling and electric market.

XINHONG WU received the B.Eng. degree in electrical engineering and the M.Eng. degree in automation of electric power systems from Zhejiang University, Hangzhou, China, in 2001 and 2007, respectively. His research interests include power system operation and electricity market.